Published in "Journal of Natural Products 81 (6): 1301–1310, 2018"
which should be cited to refer to this work.

Structures and Activities of Tiahuramides A–C, Cyclic Depsipeptides from a Tahitian Collection of the Marine Cyanobacterium *Lyngbya majuscula*

Annabel Levert,[†,□,#] Rebeca Alvariño,[‡,#] Louis Bornancin,[†,#] Eliane Abou Mansour,[†,▽] Adam M. Burja,[§,○] Anne-Marie Genevière,[⊥] Isabelle Bonnard,[†,∥] Eva Alonso,[‡] Luis Botana,[‡] and Bernard Banaigs*[,†,∥]

[†]CRIOBE, USR CNRS-EPHE-UPVD 3278, Université de Perpignan, 66860 Perpignan, France

[‡]Departamento de Farmacología, Facultad de Veterinaria, Universidad de Santiago de Compostela, Lugo 27003, Spain

[§]Heriot-Watt University, Edinburgh, Scotland EH14 4 AS

[⊥]Biologie Intégrative des Organismes Marins (BIOM), Sorbonne Universités, UPMC Univ Paris 06, CNRS, Observatoire Océanologique, F-66650, Banyuls/Mer, France

[∥]Laboratoire d'Excellence "CORAIL", 66860, Perpignan, Cedex, France

S *Supporting Information*

ABSTRACT: The structures of three new cyclic depsipeptides, tiahuramides A (**1**), B (**2**), and C (**3**), from a French Polynesian collection of the marine cyanobacterium *Lyngbya majuscula* are described. The planar structures of these compounds were established by a combination of mass spectrometry and 1D and 2D NMR experiments. Absolute configurations of natural and nonproteinogenic amino acids were determined through a combination of acid hydrolysis, derivitization with Marfey's reagent, and HPLC. The absolute configuration of hydroxy acids was confirmed by Mosher's method. The antibacterial activities of tiahuramides against three marine bacteria were evaluated. Compound **3** was the most active compound of the series, with an MIC of 6.7 μM on one of the three tested bacteria. The three peptides inhibit the first cell division of sea urchin fertilized eggs with IC_{50} values in the range from 3.9 to 11 μM. Tiahuramide B (**2**), the most potent compound, causes cellular alteration characteristics of apoptotic cells, blebbing, DNA condensation, and fragmentation, already at the first egg cleavage. The cytotoxic activity of compounds **1**–**3** was tested in SH-SY5Y human neuroblastoma cells. Compounds **2** and **3** showed an IC_{50} of 14 and 6.0 μM, respectively, whereas compound **1** displayed no toxicity in this cell line at 100 μM. To determine the type of cell death induced by tiahuramide C (**3**), SH-SY5Y cells were costained with annexin V–FITC and propidium iodide and analyzed by flow cytometry. The double staining indicated that the cytotoxicity of compound **3** in this cell line is produced by necrosis.

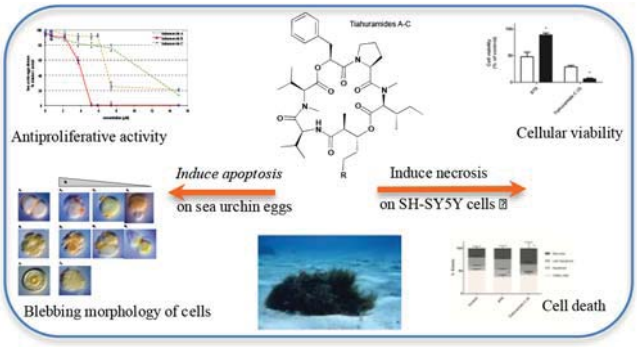

Through the pioneering work of Richard Moore[1] and others,[2] marine cyanobacteria have emerged as one of the richest groups of marine microorganisms in terms of both structural diversity and biological activity of the associated secondary metabolites. Studies of these microorganisms highlight a few species as being prolific sources of natural products, with members of the Oscillatoriaceae, especially the marine filamentous cyanobacterium *Lyngbya majuscula* Harvey ex Gomont, being predominant.[3] Among others, *L. majuscula* was found to produce a variety of cyclic peptides such as somamides,[4] antillatoxins,[5] homodolastatin 16,[6] wewakazole,[7] lyngbyastatins,[8] lyngbyabellins,[9] or apratoxin A.[10] Within these lipocyclopeptides, a series of cyclic penta-, hexa-, or heptadepsipeptides containing two ester linkages and a methyl or dimethylhydroxyoctynoic acid residue such as yanucamides,[11] antanapeptins,[12] pitipeptolides,[13] trungapeptins,[14] hantupeptins,[15] and lagunamides[16] are also well represented. All of these compounds are structurally related, and most of them have been reported to possess cytotoxic activities against cancer cells.

We report here the isolation and characterization of three new cyclohexadepsipeptides, tiahuramides A (**1**), B (**2**), and C (**3**), from *L. majuscula* collected at Tiahura Atoll, Moorea Island (French Polynesia). Their structures were deduced by extensive LC-MS analysis, 1D and 2D NMR spectrometry, and characterization of degradation products. These compounds are new members of the NRPS–PKS peptide family and in a subfamily containing a fatty acid moiety within an overall cyclic

Table 1. NMR Assignments (^{1}H 400 MHz, ^{13}C 100 MHz, $CDCl_3$) for Tiahuramides A (1), B (2), and C (3)

		tiahuramide A (1)		tiahuramide B (2)		tiahuramide C (3)	
	position	δ_C, type	δ_H (J in Hz)	δ_C, type	δ_H (J in Hz)	δ_C, type	δ_H (J in Hz)
Hmoya/Hmoea/Hmoaa	1	170.9, C		171.0, C		171.2, C	
	2	42.2, CH	3.25, qd (7.5, 2.2)	42.3, CH	3.25	42.3, CH	3.24
	3	76.7, CH	4.88, td (10.5, 2.2)	77.2, CH	4.87	77.2, CH	4.86
	4	27.5, CH_2	1.63, 2.06	28.4, CH_2	1.79	28.7, CH_2	1.80
	5	25.2, CH_2	1.47	25.6, CH_2	1.61	26.1, CH_2	1.59
	6	18.0, CH_2	2.18	33.2, CH_2	2.04	31.4, CH_2	1.31
	7	83.5, C		138.1, CH	5.73	22.5, CH_2	1.40
	8	68.9, CH	1.92,t(2.5)	114.9, CH	4.93, 4.97	13.9, CH	0.89
	9	14.5, CH_3	1.27,d(7.4)	14.5, CH_3	1.24	14.4, CH_3	1.25
Val	10	173.4, C		173.5, C		173.5, C	
	11	52.8, CH	4.74, dd (8.5, 6.5)	52.8, CH	4.75	52.8, CH	4.75
	12	32.3, CH	1.96	32.3, CH	1.96	32.3, CH	1.95
	13	17.7, CH_3	0.86	17.7, CH_3	0.86	17.7, CH_3	0.86
	14	20.3, CH_3	0.88	20.2, CH_3	0.88	20.2, CH_3	0.88
	NH		6.24, d (8.5)		6.23		6.23
N-Me-Val	15	168.9, C		168.8		168.8	
	16	65.8, CH	4.07, d (10.2)	65.8	4.08	65.8	4.08
	17	27.4, CH	2.08	27.4	2.07	27.4	2.06
	18	19.8, CH_3	0.86	19.7	0.86	19.7	0.85
	19	20.0, CH_3	0.92	20.0	0.92	20.0	0.90
	20	29.0, CH_3	2.54	29.0	2.52	29.0	2.52
	21	165.4, C		165.5		165.4	
Pla	22	72.8, CH	5.48, dd (9.5, 4.1)	72.7	5.49	72.7	5.49
	23	36.7, CH_2	3.14, dd (15.0, 4.1)	36.7	3.14	36.7	3.14
			2.88, dd (15.0, 9.5)		2.88		2.87
	24	136.2, C		136.2		136.2	
	25/29	129.3, CH	7.16	129.4	7.15	129.4	7.15
	26/28	128.5, CH	7.26	128.5	7.26	128.5	7.25
	27	126.7, CH	7.15	126.8	7.14	126.7	7.15
Pro	30	172.4, C		172.5		172.5	
	31	57.2, CH	4.94, dd (8.8,4.5)	57.2	4.97	57.2	4.95
	32	29.1, CH_2	1.79, 2.26	29.1	2.28, 1.77	29.1	2.24, 1.80
	33	25.1, CH_2	1.92, 2.06	25.1	2.05, 1.95	25.1	2.06, 1.95
	34	47.0, CH_2	3.55, m	47.0	3.54	47.0	3.54
N-Me-Ile	35	170.8, C		170.9		170.9	
	36	64.1, CH	4.01, d (10.8)	64.2	4.03	64.2	4.02
	37	34.6, CH	2.03, m	34.6	2.04	34.6	2.05
	38	25.7, CH_2	1.45, m	25.7	1.47	25.8	1.46
	39	11.1, CH_3	0.93, t	11.1	0.92	11.1	0.91
	40	15.8, CH_3	0.94, d	15.8	0.94	15.7	0.93
	41	28.8, CH_3	3.03	28.9	3.04	28.8	3.04

depsipeptide framework. The ecological activities of the three new compounds were evaluated against marine bacteria and sea urchin eggs. Constrained stable peptide scaffolds with a lipid tail for membrane association are considered as potential new drugs, but connecting structure to function is notoriously difficult; the pharmacological activities of the three new compounds were also evaluated against human pathogenic bacteria and human neuroblastoma cells.

RESULTS AND DISCUSSION

This specimen of *L. majuscula* was collected by scuba from the shallow lagoon complex surrounding Tiahura Atoll. The EtOAc extract of the freeze-dried material (100 g) was subjected to repeated reversed-phase chromatography to afford three new lipopeptides, tiahuramides A–C (**1**–**3**). The tiahuramides were obtained as colorless, amorphous solids. The IR spectra indicated the presence of both ester (1735 cm^{-1}) and amide (1645 cm^{-1}) functionalities. Various features of the ^{1}H and ^{13}C NMR data (Table 1) suggested lipopeptidic structures. The tiahuramides were negative to the ninhydrin test, suggesting a blocked N-terminus. The three metabolites exhibited very similar ^{1}H and ^{13}C NMR data. Tiahuramides B (**2**) and C (**3**) differed, in high-resolution mass spectrometry, from tiahuramide A (**1**) by 2 and 4 amu's, respectively.

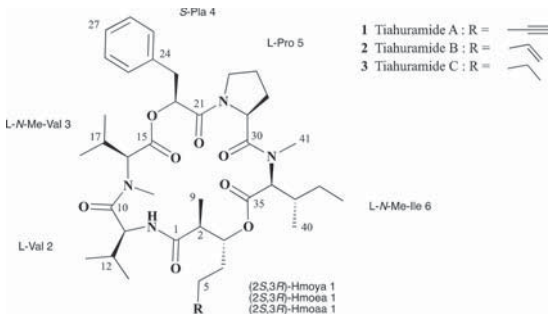

The most abundant of these metabolites was tiahuramide A (**1**); the molecular formula was established as $C_{41}H_{60}N_4O_8$

from positive high-resolution MS (obsd $[M + H]^+$ at m/z 737.4472). The NMR profiles were complex due to the presence of a mixture of conformers in slow exchange. The conformational equilibrium was observed in all solvents used (CD_2Cl_2, $CDCl_3$, DMSO-d_6), and variable-temperature NMR analysis, ranging from 293 to 333 K, did not improve this feature. NMR was finally recorded at 298 K in $CDCl_3$, where one conformation strongly dominates, in an approximate ratio of 13:2:1:1. The structure elucidation was based on NMR analysis of the major conformer.

Six partial structures could be assembled by detailed analysis of one- and two-dimensional NMR spectra. A combination of COSY, HOHAHA, HSQC, and HMBC NMR experiments indicated the presence of four standard amino acid residues, one valine (Val), one proline (Pro), two *N*-methylated amino acids, *N*-methylvaline (*N*-Me-Val), and *N*-methylisoleucine (*N*-Me-Ile), and two hydroxy acids. The first one exhibited signals in the ^{1}H NMR spectrum attributable to a phenylalanine with resonances at 7.16−7.26 (H-25/H-29 and H-26/H-28), 5.48 (H-22), 3.14, and 2.88 ppm (H-23). The chemical shift of the C-22 (72.8 ppm) was that of an oxymethine, indicating that this residue is 3-phenyllactic acid (Pla). The structure of the second hydroxy acid was deduced as follows: a methine group ^{1}H/^{13}C NMR (δ 3.25/42.2, H-2/C-2) is connected to a carbonyl group (δ 170.9, C-1), to a methyl group (δ 1.27/14.5, H_3-9/C-9), and to an oxygen-bearing methine (δ 4.88/76.7, H-3/C-3) which is bonded to a chain formed by three methylenes (δ 2.06−1.63/27.5, H_2-4/C-4; δ 1.47/25.2, H_2-5/C-5; δ 2.18/18.0, H_2-6/C-6), the last one being connected to a terminal acetylene (δ 83.5, C-7; 1.92/68.8, H-8). This identified the residue as 3-hydroxy-2-methyloct-7-ynoic acid (Hmoya). The two hydroxy acid residues, Pla and Hmoya, have previously been reported within other peptide structures isolated from other cyanobacteria or organisms that are known to graze on cyanobacteria.

Sequencing of these residues was performed by HMBC and ROESY analyses. The partial sequences Hmoya−Val−*N*-Me-Val−Pla and Pro−*N*-Me-Ile could be deduced from HMBC correlations between NHVal/COHmoya; NCH_3, HαMe-Val/COVal; H-22Pla/COMe-Val and NCH_3; and HαMe-Ile/COPro. A ROESY correlation between H-22Pla and HδPro linked the two moieties leading to the sequence Hmoya−Val−*N*-Me-Val−Pla−Pro−*N*-Me-Ile. As is the case for the antanapeptins or kulomo'opunalide 1,[17] two closely related cyclohexadepsipeptides, the linkage cyclizing the molecule through the ester bond between Hmoya and N-Me-Ile could not be observed in either the HMBC or ROESY spectra.

Evidence for this linkage, the only possibility to satisfy the molecular formula, was found by evaluating the NOE data; the Hα*N*-Me-Ile (δ 4.01) showed a weak NOE cross-peak with one of the two diastereotopic H-4 (δ 2.06) of the Hmoya residue (Figure 1). The mass spectrometric fragmentation pattern of the tiahuramides observed by positive-mode ESI $(MS)^n$ confirmed the sequence derived from NMR experiments (Figure 2). Formation of a sodium adduct ion at m/z 759 $[M + Na]^+$ was followed by ring cleavage to form the linear acylium ion with *N*-Me-Ile at the C-terminus. This acylium ion underwent a C-terminus fragmentation.

High-resolution MS of tiahuramide B (**2**) established its molecular formula as $C_{41}H_{62}N_4O_8$ (obsd $[M + H]^+$ at m/z 739.4624), two mass units higher than that of tiahuramide A (**1**). In collisionally induced tandem ESIMS, the mass fragmentation pattern of **2** (Figure 2) showed that the 2 amu difference is observable after successive losses of *N*-Me-Ile, Pro,

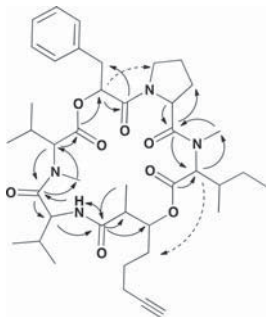

Figure 1. HMBC and dipolar (NOESY or ROESY) correlations. The key dipolar correlations that suggest the Pla−Pro and N-Me-Ile-Hmoya linkages are indicated by dashed lines.

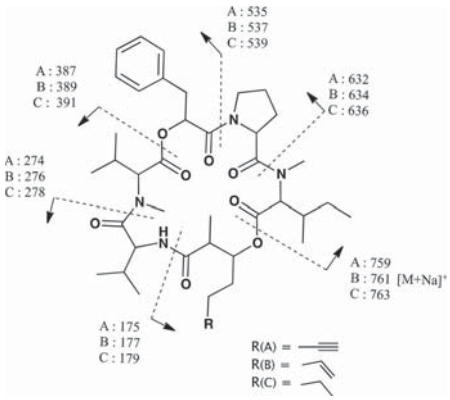

Figure 2. Mass spectrometric fragmentation of tiahuramides A, B, and C.

Pla, *N*-Me-Val, and Val residues. The only obvious differences in the ^{1}H NMR spectrum of tiahuramide B (**2**) were the missing acetylenic resonance and the appearance of three olefinic proton signals (δ 5.73, 4.97, and 4.93) (Table 1). In the ^{13}C NMR spectrum, the signals at 83.5 (C-7) and 68.9 ppm (C-8) for the Hmoya unit in **1** were shifted to δ 138.1 and 114.9 ppm and were found to be consistent with the partial reduction of the terminal triple bond to a double bond. Therefore, 2D NMR analyses confirmed that the change had taken place on the 3-hydroxy-2-methyloct-7-ynoic acid (Hmoya), where it has been replaced by 3-hydroxy-2-methyloct-7-enoic acid (Hmoea).

Furthermore, high-resolution MS of tiahuramide C (**3**) established its molecular formula as $C_{41}H_{64}N_4O_8$, corresponding to four mass units higher than that of tiahuramide A (**1**) (obsd $[M + H]^+$ at m/z 741.4781). The acetylenic carbons were absent from the ^{13}C NMR spectrum and were replaced by two additional shielded carbons at δ 22.5 (C-7) and 13.9 (C-8). Analysis of 1D and 2D NMR data of **3** indicated that 3-hydroxy-2-methyloct-7-ynoic acid (Hmoya) in **1** is replaced by 3-hydroxy-2-methyloct-7-anoic acid (Hmoaa) in **3**. Concerning the relative configuration of C-2 and C-3 of the Hmoya unit, the observed $^3J_{H2-H3}$ value of 2.2 Hz was consistent with the *syn* configuration at C-2 and C-3.[14] The relative configuration in compounds **2** and **3**, due to very similar ^{13}C and ^{1}H chemical shifts of all residues in the tiahuramides, was assumed to be the same as in **1**. Thus, except for the Hmoya-terminal side chain (C-4 to C-8), the maximum difference is 0.03 ppm for the ^{1}H NMR data [Hα and HγPro[5] **2** vs **1**, HγPro[5] **3** vs **1**] and 0.1 ppm for the ^{13}C NMR data [CO *N*-MeIle[6] and CδPla[3] **2** vs **1**, Cγ *N*-MeIle[6]].

The absolute configurations of stereocenters of tiahuramides were established by applying various chemical and spectroscopic

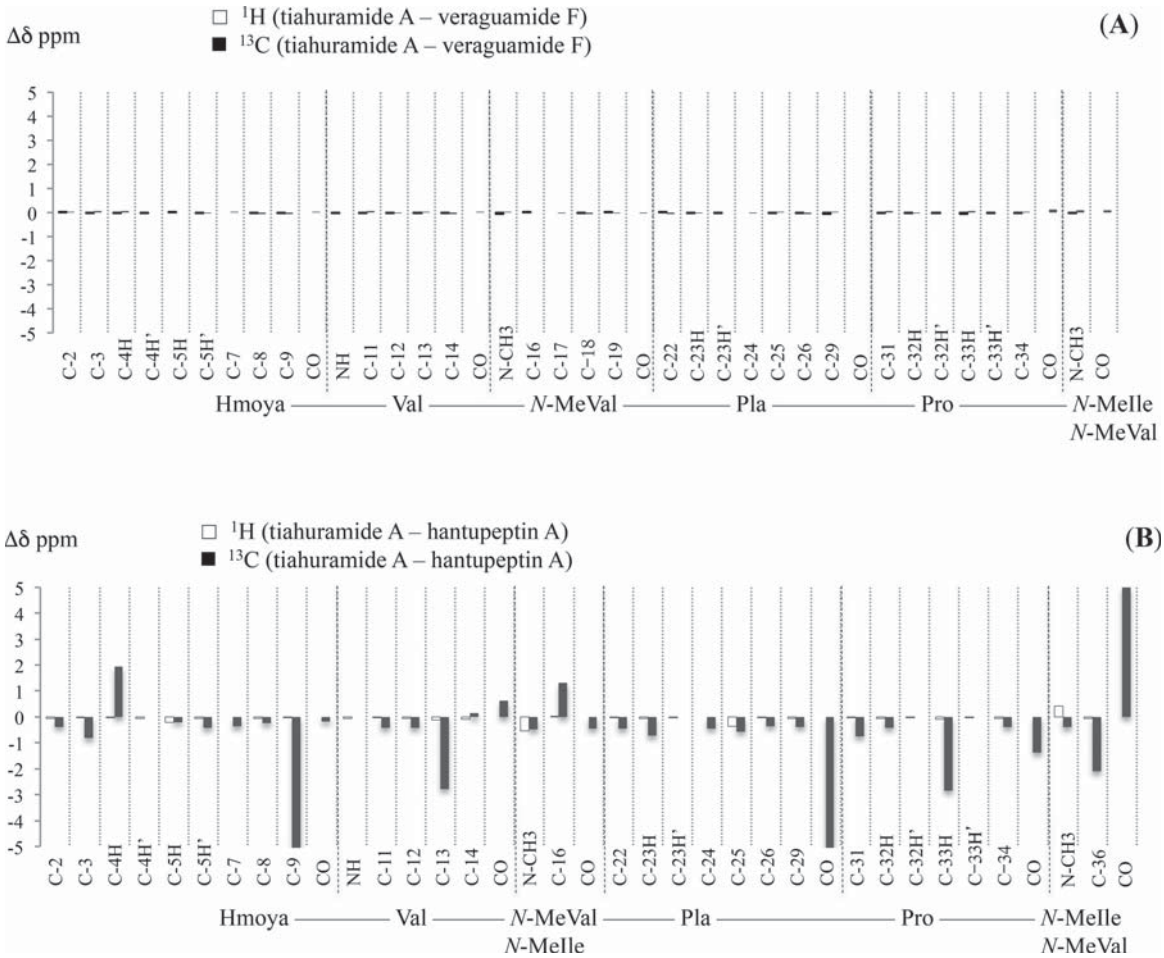

Figure 3. Chemical shift changes ($\Delta\delta$) for tiahuramide A relative to veraguamide F (A) and hantupeptin A (B). $\Delta\delta$ is calculated by subtracting the chemical shift of ^{1}H and ^{13}C resonances of tiahuramide A from that of veraguamide F or hantupeptin A.

methods based on the chemical properties of these cyclodepsipeptides. Stereochemical assignments of the amino acids in **1** were based on the advanced Marfey's method coupled with LC-MS analysis[18] of the acid hydrolysate, revealing the absolute configurations of Val^{2}, *N*-Me-Val^{3}, Pro^{5}, and *N*-Me-Ile^{6} to be L. In order to rule out *N*-Me-*allo*-Ile, the hydrolysate of **1** was compared to L-Marfey derivatized *N*-Me-L-Ile and *N*-Me-D-*allo*-Ile standards. The identical retention times of the L-Marfey derivatized *N*-Me-L-Ile standard and the *N*-Me-Ile unit in the hydrolysate confirmed an L-configuration of the *N*-Me-Ile moiety. Tiahuramide A was also subjected to methanolysis, resulting in the isolation of two fragments, HO-Hmoya−Val−*N*-Me-Val-OCH_3 and HO-Pla−Pro−*N*-Me-Ile-OCH_3, the structures of which where confirmed by HRMS and ^{1}H NMR. Subsequent treatment of the two fragments with Mosher's reagent showed that C-22 Pla was *S* and C-3 Hmoya was *R*.

The tiahuramides likely derive from a mixed NRPS−PKS biosynthetic pathway; they join the kulolide superfamily described by Boudreau et al.[19] In this family the configurations of the different residues are highly conserved. Starting from Hmoya^{1} toward the C-terminal part *N*-Me-Ile^{6}, the consecutive configurations of the carbon atoms constituting the macrocycle are as follows: *S*−*R*−*S*−*S*−*S*−*S*−*S*. The only exception, for now, are hantupeptins A−C, with a sequence *R*−*S*−*S*−*S*−*S*−*S*−*S*. In tiahuramide A (**1**), the configurations of the C-2, C-3, and C-22 stereocenters in the hydroxy acids, Hmoya and Pla, have been determined to be 2*S*,3*R*-Hmoya and *S*-Pla, leading to a *S*−*R*−*S*−*S*−*S*−*S*−*S* sequence. Conservation of configurations of the carbon atoms constituting the macrocycle can be analyzed by comparison of the ^{1}H and ^{13}C chemical shifts of tiahuramide A with the closely related compounds veraguamide F [2*S*,3*R*-Hmoya^{1}−L-Val^{2}−L-*N*-Me-Val^{3}−*S*-Pla^{4}−L-Pro^{5}−L-*N*-Me-Val^{6}] and hantupeptin A [2*R*,3*S*-Hmoya^{1}−L-Val^{2}−L-*N*-Me-Ile^{3}−*S*-Pla^{4}−L-Pro^{5}−L-*N*-Me-Val^{6}], tiahuramide A differing in the sequence from veraguamide F (*S*−*R*−*S*−*S*−*S*−*S*−*S* sequence) by the replacement of L-*N*-Me-Ile^{6} by L-*N*-Me-Val^{6}, and tiahuramide A from hantupeptin A (*R*−*S*−*S*−*S*−*S*−*S*−*S* sequence) by the inversion of residues 3 and 6 (L-*N*-MeVal^{3}/L-*N*-MeIle^{3} and L-*N*-Me-Ile^{6}/L-*N*-Me-Val^{6}). Indeed in these small cyclic peptides, conformational mobility is greatly restricted and NMR *chemical shifts* are highly dependent on the Cα configuration of the peptidic backbone.

Tiahuramide A showed very similar NMR chemical shifts to veraguamide F for the peptidic backbone as well as for the side chains, suggesting the same configurations and very closely related conformations. An indication of this similarity could be seen graphically in Figure 3A, where the ^{1}H and ^{13}C backbone and side chain resonances of veraguamide F were subtracted from the equivalent ones of tiahuramide A. With the exception of the structurally modified *N*-Me-Ile^{6}/*N*-Me-Val^{6} side chain (not shown in the figure), all of the ^{1}H and ^{13}C resonances had similar chemical shifts in both compounds: the maximum difference observed was less than 0.06 ppm in ^{1}H and less than 0.1 ppm in ^{13}C. In the comparison tiahuramide A vs hantupeptin A,

S–*R*–*S*–*S*–*S*–*S*–*S* sequence vs *R*–*S*–*S*–*S*–*S*–*S*–*S* sequence, the differences are much larger (more than 0.4 ppm in ^{1}H and 5 ppm in ^{13}C) (Figure 3B). The same comparison can be made (data not shown) with tiahuramides B (**2**) and C (**3**) with the same conclusions: the absolute configurations of the amino acids Val^{2}, *N*-Me-Val^{3}, Pro^{5}, and *N*-Me-Ile^{6} in **2** and **3** are L, and the two hydroxy acids Hmoea, in **2**, and Hmoaa, in **3** and Pla, are respectively 2*S*,3*R* and *S* as in tiahuramide A (**1**).

Therefore, the complete structure of the two new compounds can be reasonably proposed as

- tiahuramide A (**1**): 2*S*,3*R*-Hmoya^{1}–L-Val^{2}–L-*N*-Me-Val^{3}–*S*-Pla^{4}–L-Pro^{5}–L-*N*-Me-Ile^{6}
- tiahuramide B (**2**): 2*S*,3*R*-Hmoea^{1}–L-Val^{2}–L-*N*-Me-Val^{3}–*S*-Pla^{4}–L-Pro^{5}–L-*N*-Me-Ile^{6}
- tiahuramide C (**3**): 2*S*,3*R*-Hmoaa^{1}–L-Val^{2}–L-*N*-Me-Val^{3}–*S*-Pla^{4}–L-Pro^{5}–L-*N*-Me-Ile^{6}

Finally, in addition to the three new compounds isolated and elucidated here, this particular collection of *L. majuscula* was found to contain several other previously identified natural products, identified via NMR and high-resolution MS. These were malyngamide C, two serinol-derived malyngamides, dolastatin 16, and trungapeptins A–C.[14]

Biological Evaluation of Tiahuramides. *Antibacterial and Antifouling Activities of Tiahuramides.* We determinated the antibacterial activities of tiahuramides against three opportunistic marine pathogenic bacteria, *Aeromonas salmonicida*, *Vibrio anguillarum*, and *Shewanella baltica*. The three strains were selected because they have been implicated in the first step of marine biofouling in addition to their pathogenic interest.[20] Thus, the antimicrobial assays provide an estimate of the antifouling and antimicrobial potential of tiahuramides. The antibacterial activity was evaluated by the microtiter broth dilution method.[21] The bacteria (*A. salmonicida*, *V. anguillarum*, and *S. baltica*) were incubated with increasing concentrations of tiahuramides in 96-well microplates. Results are shown in Table 2.

Table 2. Minimum Inhibitory Concentration (MIC) of Tiahuramides against the Marine *Aeromonas salmonicida*, *Vibrio anguillarum*, and *Shewanella baltica* and the Terrestrial *Escherichia coli and Micrococcus luteus* Bacteria

	MIC (μM)				
	A. salmonicida	*V. anguillarum*	*S. baltica*	*E. coli*	*M. luteus*
tiahuramide A (**1**)	27	33	>50	35	47
tiahuramide B (**2**)	9.4	8.5	22	12	29
tiahuramide C (**3**)	6.7	7.4	16	14	17

Tiahuramide A is the least active compound of the series, with MIC values of 27 and 33 μM against *A. salmonicida* and *V. anguillarum*, respectively, and does not inhibit the growth of *S. baltica*. Tiahuramide C is the most active compound of the series, with MIC values of 7, 7, and 16 μM against *A. salmonicida*, *V. anguillarum*, and *S. baltica*, respectively.

Antibacterial assays were also carried out on Gram-negative (*Escherichia coli*) and Gram-positive (*Micrococcus luteus*) bacteria. Results are shown in Table 2. Tiahuramides A–C inhibit moderately the growth of *E. coli* and *M. luteus* (Table 2). Tiahuramide A is the least active compound of the series. Tiahuramides B and C have similar values of MIC because they inhibit the growth of the two bacterial strains between 12 and 29 μM.

Antiproliferative Activity on Sea Urchin Eggs. We investigated the ability of the three peptides to inhibit the first cell division of *Paracentrotus lividus* eggs. Gametes were collected after acetylcholine injection into the coelomic cavity. Fertilization was performed as described in the Experimental Section. Fertilized eggs were incubated in the presence of increasing concentrations of tiahuramides, from 0 to 30 μM, in 96-well microplates. Eggs were observed under an inverted microscope, and the percentages of dividing eggs were recorded 75 min postfertilization (p.f.) when control eggs have completed the first cleavage.

The three compounds exhibit a dose-dependent effect on the first cell division of sea urchin eggs as indicated in Figure 4.

Tiahuramide B was the most active compound of the series. When fertilized eggs were incubated with tiahuramide B at 2 and 4 μM, respectively, 10% and 60% of the eggs did not divide 75 min p.f. Above 5 μM, no division was observed. The calculated IC_{50} of tiahuramide B is 3.9 μM on *P. lividus* egg division (11 μM for tiahuramide A and 7 μM for tiahuramide C).

Tiahuramide B, as the most potent compound, was selected to carefully examine the morphology of *P. lividus* fertilized eggs over 18 h, a time when control embryos have reached the blastula stage (Figure 5). Fertilized eggs were incubated with 5 μM tiahuramide B and observed under an optical microscope (Figure 5 A2–A4; B2–B4; C2). Control eggs (Figure 5A1, B1, and C1) were incubated under the same conditions (with seawater containing 1% MeOH).

Control eggs are at the two-cell stage 80 min after fertilization (Figure 6, A1). Eggs incubated with 5 μM tiahuramide B did not divide (Figure 5, A2 and A3), and we can observe granulations of the plasmic membrane. A small percentage (8%) of the eggs divided in an abnormal way (Figure 5, A4), with the formation of extracellular cytoplasmic granules.

Control eggs are at the 16-cell stage 120 min after fertilization (Figure 6, B1). Eggs treated with 5 μM tiahuramide B presented abnormal phenotypes with the same morphology as eggs observed 80 min after fertilization, i.e., granulation of the membrane (Figure 5, B2 and B3). Control embryos hatched and reached the mesenchymal blastula stage 18 h p.f. (Figure 5 C1). Eggs treated with 5 μM tiahuramide B never reached this stage, cell divisions were strongly perturbed, and eggs acquired a characteristic blebbing morphology of cells undergoing apoptosis.

Apoptosis, or programmed cell death, is characterized by various morphological and biochemical criteria such as contraction of cells and blebbing, condensation and fragmentation of chromatin, an increase in the membrane permeability, and specific activation of caspases.[22] Apoptosis occurred in sea urchin eggs upon treatment with staurosporine, a kinase inhibitor, camptothecin, an inhibitor of topoisomerase II, and organotin(IV) chlorin derivatives or by alteration of cyclin B synthesis.[23]

Prominent criteria of apoptotic cell death are the condensation and fragmentation of DNA. Therefore, eggs treated with 5 μM tiahuramide B were stained with DAPI (4′,6-diamidine-2′-phenylindole dihydrochloride) in order to visualize the state of the nuclear DNA.

In control *P. lividus* eggs 30 min p.f. male and female DNA have fused and chromatin is decondensed (Figure 6 A). In contrast, in eggs treated with 5 μM tiahuramide B, chromatin remained condensed and localized at the nucleus periphery (Figure 6B). Upon cell cycle progression, condensed chromosomes aligned at the metaphase plate 60 min p.f. in control eggs (Figure 6 C), while condensed DNA was dispersed in the nucleus (Figure 6D) of treated eggs. Thus, tiahuramide B causes abnormal DNA condensation.

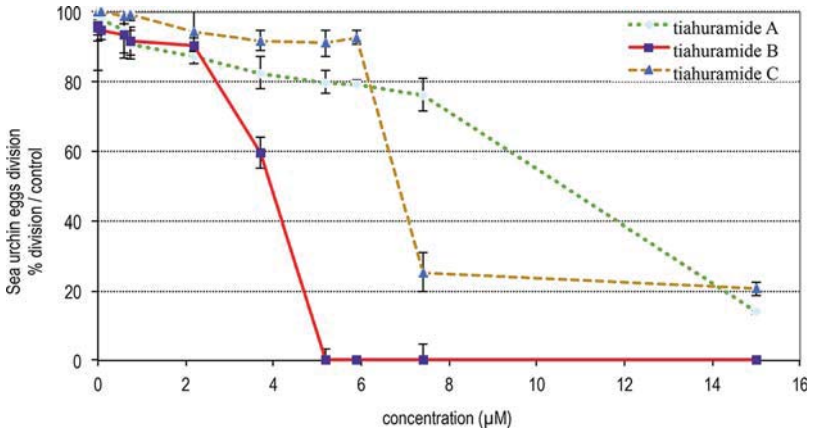

Figure 4. Fertilized eggs of *Paracentrotus lividus*, incubated with increasing concentrations of tiahuramides A–C. Percent of dividing eggs 75 min after fertilization.

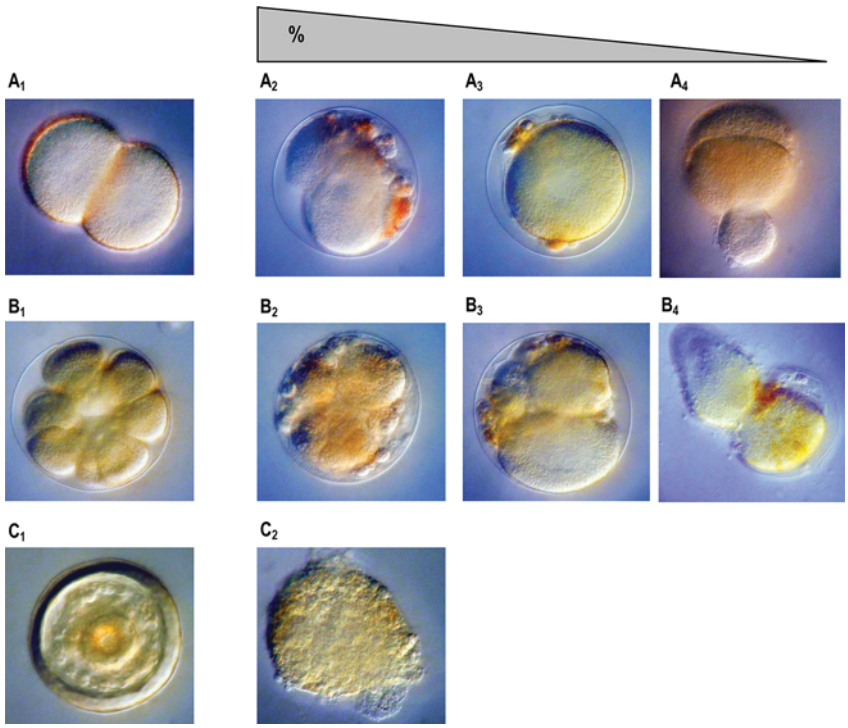

Figure 5. Fertilized eggs of *Paracentrotus lividus*, controls (A1–C1) and those incubated with 5 μM tiahuramide B (A2–A4; B2–B4; C2), and the percentage of the typical observed morphology. The morphology of eggs of *P. lividus* was observed 80 min (A1–A4), 120 min (B1–B4), and 18 h postfertilization (C1, C2) under a reversed optical microscope (20×). Scale bar: 40 μm.

We further investigated DNA fragmentation using the terminal dUTP nick end labeling (TUNEL) assay (Figure 7). Fluorescent TUNEL labeling visualizes the 3′-OH end of DNA strand breaks as a result of the activation of endonucleases in apoptotic cells.

The *P. lividus* control eggs visualized before the first cell division (60 min p.f.) (Figure 7 A) were all negative for TUNEL staining. In contrast, control eggs treated with DNase presented a strongly fluorescent nucleus (Figure 7B) correlated with the DNA fragmentation produced by DNase. Eggs treated with 5 μM tiahuramide B (Figure 7C) also present fluorescent nuclei, highlighting the fragmentation of chromatin in these eggs. Therefore, tiahuramide B causes DNA fragmentation in *P. lividus* eggs.

In summary, the three tiahuramides isolated from *L. majuscula* exhibited antiproliferative capacity on *P. lividus* eggs, with tiahuramide B (**2**) being the most active of the three compounds. Moreover tiahuramide B causes cellular alteration characteristic of apoptotic cells, blebbing, and DNA condensation and fragmentation, already at the first *P. lividus* egg division.

Cytotoxic Activity on a Human Neuroblastoma Cell Line. *In vitro* cytotoxicity of the tiahuramides was evaluated on the human neuroblastoma SH-SY5Y cell line. SH-SY5Y cells were incubated with tiahuramides A (**1**), B (**2**), and C (**3**) at concentrations ranging from 100 to 0.001 μM for 24 h, and cell viability was assessed by the MTT assay. Tiahuramide A (**1**) showed no toxicity against this cell line at any of the concentrations tested. Tiahuramides B (**2**) and C (**3**) presented IC_{50} values of 14 ± 2 and 6.0 ± 2.7 μM, respectively.

In order to better understand the cell death produced by tiahuramide C (**3**), SH-SY5Y cells were preincubated with the caspase inhibitor Z-VAD-FMK (40 μM) for 24 h. After this

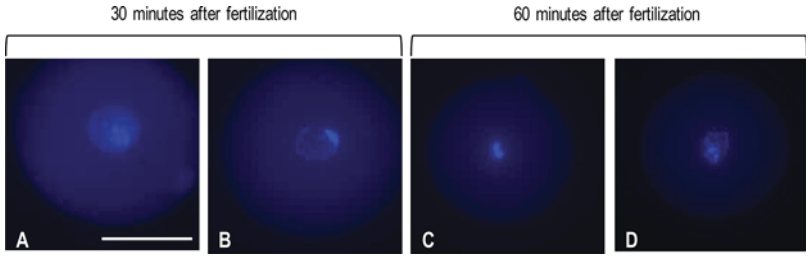

Figure 6. Effect of tiahuramide B (5 μM) on *Paracentrotus lividus* eggs. DNA of control (A and C) and treated (B and D) eggs was visualized by staining cells with DAPI 30 and 60 min after fertilization. Scale bar: 40 μm.

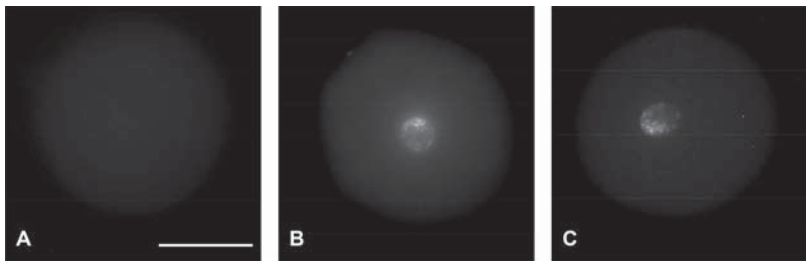

Figure 7. Fragmentation of DNA in eggs treated with DNase (B) and tiahuramide B (C). DNA of control eggs is not fragmented (A). The fluorescence of the nucleus is related to the fixation of the fluorescent nucleotides in the 3′-OH end of the DNA generated during the fragmentation. Scale: 40 μm.

time, tiahuramide C (**3**) (5, 10, and 15 μM) was added to the cells for 6 h. Staurosporine (STS, 0.5 μM), an apoptosis inducer, was used as the control. The 6 h treatment with **3** showed a decrease in cell viability only at the highest concentration. The significant difference (p = 0.04) observed between cells treated with and without Z-VAD-FMK and the compound (Figure 8) suggests that the addition of the caspase inhibitor

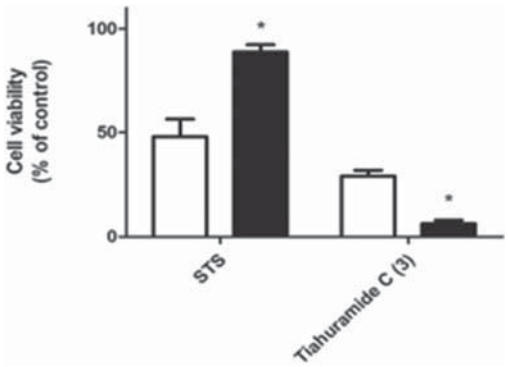

Figure 8. Cellular viability of SH-SY5Y cells co-incubated with tiahuramide C (**3**) and ZVAD-FMK. Human neuroblastoma cells were preincubated with the caspase inhibitor ZVAD-FMK for 24 h, followed by treatment with tiahuramide C (15 μM) for 6 h (black bars) and compared with cells treated only with compounds for 6 h (white bars). Staurosporine (STS, 0.5 μM) was used as an inducer of apoptosis. Cell viability was assessed by the MTT assay. Data are presented as percentage of untreated cells. Values are mean ± SEM of three independent experiments performed in triplicate. Statistical differences between cells treated with and without ZVAD-FMK were determined by Student's t test (*p < 0.05).

increases the cytotoxicity of **3**. These results indicated that the cell death produced by tiahuramide C (**3**) is not related to apoptosis in SH-SY5Y cells. On the other hand, the pretreatment with Z-VAD-FMK produced a significant increase in cell survival in the cells treated with 0.5 μM STS (p = 0.04).

In view of these results, neuroblastoma cells were stained with annexin V−FITC and propidium iodide to evaluate the type of cell death induced by **3**. SH-SY5Y cells were treated with tiahuramide C (**3**) (6.0 μM) for 6 h, and the fluorescence was analyzed by flow cytometry. The percentages of apoptotic cells (annexin V−FITC positive and propidium iodide negative), late apoptotic cells (annexin V−FITC and propidium iodide positive), and necrotic cells (annexin V−FITC negative and propidium positive) were determined. STS (1 μM) was used as a cell death control, producing a significant increase in apoptotic cells compared to control cells (p = 0.02). SH-SY5Y cells treated with tiahuramide C (**3**) showed low levels of apoptotic cell death (7.9 ± 1.4%), agreeing with the data obtained by the MTT assay. The cell death produced by **3** is mainly due to a necrotic process, with the percentage of necrotic cells being 36 ± 13% (p = 0.04) for tiahuramide C with respect to untreated cells (Figure 9).

CONCLUSION

Tiahuramides belong to a group of modified cyanobacterial peptides that consistently contain a residue with a characteristic triple-, double-, and single-bond fatty acid termination point and are the result of a mixed biogenesis involving both a polyketide synthase (PKS) and an NRPS. In this group tiahuramides A−C (**1**−**3**) belong to the kulolide superfamily defined by Boudreau et al.[22] As mentioned by those authors, the striking structural similarities within this large metabolic class suggest that the kulolide superfamily may have an ancient evolutionary origin within the cyanobacteria. Tiahuramides A−C differ from the trungapeptins by *N*-methylation of residue 5 (*N*-Me-Ile in place of Ile) and from hantupeptins A−C by inversion of the positions of residues 2 and 5.

Tiahuramides are antibacterial compounds, tiahuramides B (**2**) and C (**3**) being the most active compounds, with MIC values in the range of 6 to 29 μM. Tiahuramides also displayed cytotoxicity against sea urchin eggs and human neuroblastoma cells, with tiahuramides B and C being the most active compounds,

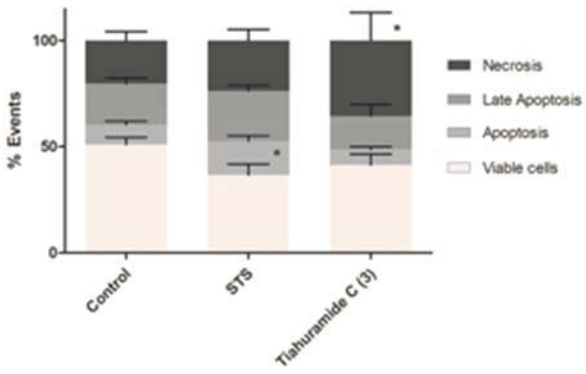

Figure 9. Analysis of cell death induced by tiahuramide C. SH-SY5Y cells were incubated with tiahuramide C (6.0 μM) for 6 h. Cells were stained with annexin−FITC and propidium iodide, and percentages of viable (annexin−FITC negative, PI negative), apoptotic (annexin−FITC positive, PI negative), late apoptotic (annexin−FITC positive, PI positive), and necrotic (annexin−FITC negative, PI positive) cells were calculated. Staurosporine (STS) at 1 μM was used as a cell death control. Values are mean ± SEM of three independent experiments and compared to control cells by Student's *t* test (*$p < 0.05$).

with IC_{50} values in the range of 4 to 14 μM. In comparison, trungapeptin A was reported to be inactive when tested at 10 μg/mL (≈14 μM) against KB and LoVo cells.[18] Hantupeptins A, B, and C were reported to be cytotoxic *in vitro* to MOLT-4 leukemia cells, with IC_{50} values of 32 nM, 0.2 μM, and 3.0 μM, respectively, and to MCF-7 breast cancer cells with IC_{50} values of 4.0 μM, 0.5 μM, and 1.0 μM, respectively.[19]

Moreover, our results suggest that tiahuramides cause eukaryotic cell death by different mechanisms: apoptosis with sea urchin eggs and necrosis with human neuroblastoma cells. These differences can be due to the phylogenetic distance between the two models. It is known, for example, that the cell death pathway that can be activated in unfertilized eggs is not the same in sea urchins and starfish, other echinoderms.[24] Therefore, differences in cell death pathways between *P. lividus* eggs and human cells are also possible, and the compounds could activate different routes. In fact, tiahuramide C (**3**) displayed the highest effects in SH-SY5Y cells, whereas in sea urchin eggs the most potent compound was tiahuramide B (**2**). On the other hand, early apoptotic cells can progress into late apoptotic cells, also known as secondary necrotic cells, when the plasma membrane becomes permeabilized.[25] Therefore, the apoptotic cell death observed in sea urchin eggs could progress to necrosis. Further experiments are needed to better understand the pathways implied in the cell death produced by tiahuramides.

EXPERIMENTAL SECTION

General Experimental Procedures. Optical rotations were determined using an Anton Paar MCP-300 polarimeter. IR and UV spectra were recorded respectively on a PerkinElmer 1600 FTIR and a Jasco V-630 spectrometer. NMR spectra were recorded on a Jeol EX 400 spectrometer with the solvent $CDCl_3$. ^1H and ^{13}C NMR chemical shifts are referenced to solvent peaks: δ_H 7.24 (residual $CHCl_3$), δ_C 77.0 for $CDCl_3$. NMR measurement conditions are indicated in the Supporting Information. Hyperaccurate mass spectra analysis was undertaken on a Bruker Q-Tof maXis mass spectrometer and LC-MS for Marfey's analyses on a Thermo LCQ-Fleet. HPLC was performed with Jasco 880-PU pumps, 7125 Rheodyne injectors, and either a Polymer Laboratories evaporative light scattering detector or a Waters 996 photodiode array detector.

Cyanobacterial Collection and Identification. The marine cyanobacteria *Lyngbya majuscula* Harvey ex Gomont (Oscillatoriaceae) (voucher specimen M98-Lm) was collected by hand from shallow waters, Tiahura sector, Moorea Island in French Polynesia (S 17°30′ W 149°50′) at a depth of 10 ft using scuba. Upon collection, samples were freeze-dried for subsequent chemical analysis in the laboratory. For morphological identification, an aliquot was taken and preserved in a solution of buffered formaldehyde in seawater (3%). The specimen was identified as *Lyngbya majuscula* Harvey ex Gomont (Hoffmann & Demoulin 1991).[26] For molecular analyses, subsamples of the field collection were stored in EtOH at room temperature and then at 4 °C before DNA extraction. The comparison of the genomic 16S rDNA sequence (GenBank accession number MG575753) with the NCBI BLAST database led to the identification of *Lyngbya majuscula* (99% identity).[27]

Extraction and Isolation of Tiahuramides A−C (1−3). Approximately 100 g of freeze-dried cyanobacteria was extracted via repetitive steeping in EtOAc, followed by separation via flash RP18 silica gel column eluting with a solvent gradient of H_2O−MeOH. Fractions were then weighed and visualized via thin-layer chromatography (TLC). Pure tiahuramides A (**1**) (7 mg), B (**2**) (4 mg), and C (**3**) (3 mg) were obtained from 160 mg of EtOAc extract, by repetitive reversed-phase HPLC using MeOH−H_2O (88:12) (Uptisphère UP5ODB column, 250 × 10 mm, 5 μm particule size, flow rate 3 mL min^{-1}, UV detection at 230 nm).

*Tiahuramide A (**1**):* white, amorphous solid; $[\alpha]^{25}_D$ −44.1 (*c* 1.5, MeOH); UV (MeOH) λ_{max} (log ε) 202 (4.4) nm; IR ($CHCl_3$) 3400 (br), 2935, 2873, 1730, 1645 (br) cm^{-1}; ^1H NMR (400 MHz, $CDCl_3$) and ^{13}C NMR (100 MHz, $CDCl_3$), Table 1; HRMS *m/z* $[M + H]^+$ 737.4472, $[M + Na]^+$ 759.4295 (calcd for $C_{41}H_{61}N_4O_8^+$, 737.4484, and for $C_{41}H_{60}N_4NaO_8^+$, 759.4303).

*Tiahuramide B (**2**):* white, amorphous solid; $[\alpha]^{25}_D$ −44.6 (*c* 1.15, MeOH); UV (MeOH) λ_{max} (log ε) 203 (4.5) nm; IR ($CHCl_3$) 3400 (br), 2932, 2871, 1730, 1644 (br) cm^{-1}; ^1H NMR (400 MHz, $CDCl_3$) and ^{13}C NMR (100 MHz, $CDCl_3$), Table 1; HRMS *m/z* $[M + H]^+$ 739.4624, $[M + Na]^+$ 761.4447 (calcd for $C_{41}H_{63}N_4O_8^+$, 739.4640, and $C_{41}H_{62}N_4NaO_8^+$, 761.4460).

*Tiahuramide C (**3**):* white, amorphous solid; $[\alpha]^{25}_D$ −40.8 (*c* 1.59, MeOH); UV (MeOH) λ_{max} (log ε) 203 (4.5) nm; IR ($CHCl_3$) 3401 (br), 2930, 2870, 1730, 1645 (br) cm^{-1}; ^1H NMR (400 MHz, $CDCl_3$) and ^{13}C NMR (100 MHz, $CDCl_3$), Table 1; HRMS *m/z* $[M + H]^+$ 741.4781, $[M + Na]^+$ 763.4605 (calcd for $C_{41}H_{65}N_4O_8^+$, 741.4797, and $C_{41}H_{64}N_4NaO_8^+$, 763.4616).

Advanced Marfey's Analysis. The Marfey's analyses were carried out on tiahuramide A. Approximately 0.4 mg of compound was hydrolyzed with 0.5 mL of 6 N HCl for 14 h at 115 °C in a sealed glass vial. The cooled hydrolysate mixture was evaporated to dryness, and traces of HCl were removed from the reaction mixtures by repeated evaporation. The hydrolysate mixture was dissolved in H_2O (100 μL) and divided into two equal aliquots. Acetone (110 μL), $NaHCO_3$ 1 N (20 μL), and 1% L- or D/L-FDLA (1-fluoro-2,4-dinitrophenyl-5-L-leucinamide) (20 μL) in acetone were added to each 50 μL aliquot. The mixtures were then heated to 40 °C for 1 h. The cooled solutions were neutralized with 1 N HCl (20 μL) and then dried *in vacuo*. The residues were dissolved in 1:1 CH_3CN−H_2O and then analyzed by LC-MS. LC-MS analyses were performed on a reversed-phase column (ThermoHypersil Gold C-18, 150 × 2.1 mm, 3 μm) with a gradient from 10% CH_3CN−90% 0.01 M formic acid to 50% CH_3CN−50% 0.01 M formic acid at 0.3 mL/min over 70 min, then to 80% CH_3CN−20% over 10 min. The configuration of the α-carbon for each residue can be assigned in accordance with the elution order of the L- and D-FDLA derivatives: amino acids for which the L-FDLA analogue elutes first have an L configuration, while those for which the D-FDLA analogue elutes first have a D configuration.[18] Retention times and ESIMS extracted ions of L-FDLA tiahuramide A hydrolysate (t_R, min, *m/z* $[M + H]^+$) were observed to be L-FDLA-Pro (36.37, 410.09), L-FDLA-Val (41.61, 411.96), and L-FDLA-*N*-Me-Val (47.38, 426.09). Retention times and ESIMS extracted ions of L/D-FDLA tiahuramide A hydrolysate (t_{R1}/t_{R2}, min, *m/z* $[M + H]^+$) were observed to be L/D-FDLA-Pro (36.34/41.33, 410.1), L/D-FDLA-Val (41.62/53.46, 411.9), and L/D-FDLA-*N*-Me-Val (47.40/54.13, 426.1). Peaks that eluted with a shorter t_R could be attributed to the L-FDLA derivatives.

Consequently, the absolute configuration of Pro, Val, and *N*-Me-Val in the hydrolysate of **1** was determined as L (see Figure S6).

In order to rule out *N*-Me-*allo*-Ile, Boc-*N*-methyl-L-isoleucine and Boc-*N*-methyl-L-*allo*-isoleucine (obtained from Chem-Impex International) were deprotected with trifluoroacetic acid in CH_2Cl_2. After solvent and acid evaporation, the amino acids were coupled to L- or L/D-FDLA using the protocol used for advanced Marfey's analyses mentioned above. Retention times (min) of each amino acid standards: L-FDLA-*N*-Me-L-*allo*-Ile (52.12), D-FDLA-*N*-Me-L-*allo*-Ile (59.26), L-FDLA-*N*-Me-L-Ile (51.78), D-FDLA-*N*-Me-L-Ile (59.08). Retention times (min) of *N*-Me-Ile derivatives in hydrolysate of tiahuramide A: L-FDLA-*N*-Me-Ile (51.78), D-FDLA-*N*-Me-Ile (59.10) (Table S1 and Figure S7).

Methanolysis of Tiahuramide A. A solution of tiahuramide A (8 mg) in 5% methanolic KOH (0.75 mL) was stirred for 72 h at room temperature (rt). The reaction mixture was diluted with diethyl ether (15 mL), and the organic layer was washed with brine, desiccated over anhydrous $MgSO_4$, and subsequently dried under reduced pressure. Purification of the two fragments was accomplished by reversed-phase HPLC (Phenomenex Luna PFP, 250 mm × 10 mm, H_2O–CH_3CN (65:35) + 1% HCOOH).[15a]

α-Methoxy-α-trifluoromethyl-α-phenylacetic Acid (MTPA) Esters of HO-Hmoya–Val–*N*-Me-Val-OCH_3 and HO-Pla–Pro–*N*-Me-Ile-OCH_3 Fragments. Fragments obtained from the methanolysis of tiahuramide A were divided into two equal portions (1 mg each). To each sample was added 1.8 mg of *R*- or *S*-MTPA–OH acid (7.75 μmol, 3.1 equiv), dissolved in 150 μL of CH_2Cl_2, and then DCC (dicyclohexylcarbodiimide, 1.6 mg, 7.75 μmol, 3.1 equiv) and DMAP (4-dimethylaminopyridine, 0.95 mg, 7.75 μmol, 3.1 equiv) were added. The reaction was carried out for 24 h at rt under stirring, and the solvent was evaporated under reduced pressure. The corresponding esters, MTPA-O-Hmoya–Val–*N*-Me-Val-OCH_3 and MTPA-O-Pla–Pro–*N*-Me-Ile-OCH_3, were purified by reversed-phase HPLC (Phenomenex Luna PFP, 250 mm × 10 mm, H_2O–CH_3CN (40:60) + 1% HCOOH) and subjected to NMR analysis.

(R)-MTPA-O-Hmoya–Val–N-Me-Val-OCH_3: ^{1}H NMR ($CDCl_3$) δ 2.55 (H-2 Hmoya), 2.07 (H-6 Hmoya), 1.90 (H-8 Hmoya), 1.19 (CH_3 Hmoya), 6.28 (NH Val), 5.30 (H3 Hmoya), 4.93 (Hα NMeVal), 4.73 (Hα Val), 3.69 (CH_3O), 3.55 (CH_3O), 3.06 (CH_3N Val).

(S)-MTPA-O-Hmoya–Val–N-Me-Val-OCH_3: ^{1}H NMR ($CDCl_3$) δ 2.47 (H-2 Hmoya), 2.13 (H-6 Hmoya), 1.92 (H-8 Hmoya), 1.09 (CH_3 Hmoya), 6.29 (NH Val), 5.29 (H-3 Hmoya), 4.91 (Hα NMeVal), 4.68 (Hα Val), 3.68 (CH_3O), 3.55 (CH_3O), 3.05 (CH_3N Val).

$\Delta\delta_{SR}$ H-2 Hmoya = -8×10^{-2} ppm, $\Delta\delta_{SR}$ CH_3 Hmoya = -9×10^{-2} ppm, $\Delta\delta_{SR}$ H-6 Hmoya = $+6 \times 10^{-2}$ ppm, $\Delta\delta_{SR}$ H-8 Hmoya = $+2 \times 10^{-2}$ ppm.

(R)-MTPA-O-Pla-Pro-N-Melle-OCH_3: ^{1}H NMR ($CDCl_3$) δ 5.32 (H-22 Pla), 5.06 (α Pro), 4.87 (α *N*-Me-Ile), 3.849 (δ Pro), 3.70 (CH_3O), 3.32 (CH_3O), 3.279 (H-23a Pla), 3.156 (H-23b Pla), 3.11 (CH_3N *N*-Me-Ile), 2.206 (β Pro), 2.16 (γ Pro), 2.05 (γ′ Pro), 1.895 (β′ Pro).

(S)-MTPA-O-Pla-Pro-N-Melle-OCH_3: ^{1}H NMR ($CDCl_3$) δ 5.33 (H-22 Pla), 5.05 (α Pro), 4.94 (α *N*-Me-Ile), 3.856 (δ Pro), 3.69 (CH_3O), 3.31 (CH_3O), 3.276 (H-23a Pla), 3.154 (H-23b Pla), 3.11 (CH_3N *N*-Me-Ile), 2.209 (β Pro), 2.16 (γ Pro), 2.05 (γ′ Pro), 1.900 (β′ Pro).

$\Delta\delta_{SR}$ H-23a Pla = -2×10^{-3} ppm, $\Delta\delta_{SR}$ H-23b Pla = -2×10^{-3} ppm, $\Delta\delta_{SR}$ Hδ Pro = $+7 \times 10^{-3}$ ppm, $\Delta\delta_{SR}$ Hβ Pro = $+3 \times 10^{-3}$ ppm, $\Delta\delta_{SR}$ Hβ′ Pro = $+5 \times 10^{-3}$ ppm.

Sea Urchin Embryo Cell Cycle Progression. As described in Hanssen et al.[28]

Cytotoxic Activity. The human neuroblastoma SH-SY5Y cell line was purchased from American Type Culture Collection (ATCC), number CRL2266. The cells were maintained in Dulbecco's modified Eagle's medium: Nutrient Mix F-12 (DMEM/F-12) supplemented with 10% fetal bovine serum, Glutamax, 100 U/mL penicillin, and 100 μg/mL streptomycin at 37 °C in a humidified atmosphere of 5% CO_2 and 95% air. Cells were dissociated weekly using 0.05% trypsin/EDTA. All the reagents were provided by Thermo Fisher Scientific.

The effects of tiahuramides A (**1**), B (**2**), and C (**3**) on cell viability were evaluated by the MTT (3-(4,5-dimethylthiazol-2-yl)-2,5-diphenyltetrazolium bromide) assay. One day prior to experiments, SH-SY5Y cells were seeded at a density of 5×10^4 cells per well in 96-well plates. Human neuroblastoma cells were treated with compounds at concentrations ranging from 100 to 0.001 μM for 24 h. Then, cells were rinsed with saline solution, and 200 μL of MTT (500 μg/mL) dissolved in saline buffer was added to each well. Following 1 h of incubation at 37 °C, SH-SY5Y cells were disaggregated with 5% sodium dodecyl sulfate. Absorbance of formazan crystals was measured at 595 nm with a spectrophotometer plate reader. Saponin from quillaja bark was used as a cell death control, and its absorbance was subtracted from the other data. The half-maximal inhibitory concentration (IC_{50}) was calculated by fitting the data with a log(inhibitor) vs response model of GraphPad Prism 5.0 software.

To determine if tiahuramide C (**3**) was inducing apoptosis in SH-SY5Y cells, neuroblastoma cells were seeded as described above and preincubated with 40 μM Z-VAD-FMK (Merck-Millipore) for 24 h, followed by treatment with tiahuramide C (5, 10, and 15 μM) during 6 h. Then, the MTT assay was carried out as described before.

The cell death type induced by tiahuramide C (**3**) was determined with an annexin V–FITC apoptosis detection kit (Immunostep, Spain) following the manufacturer's instructions. SH-SY5Y cells were seeded in six-well plates at 1×10^6 cells per well and incubated for 6 h with tiahuramide C (**3**) at 6 μM. Then, cells were washed with phosphate-buffered saline and resuspended in annexin binding buffer containing annexin V–FITC and propidium iodide. SH-SY5Y cells were incubated for 15 min and analyzed by flow cytometry using the ImageStream MKII (Amnis Corporation, Merck-Millipore). The fluorescence of 10 000 events was analyzed with IDEAS Application software ver. 6.0 (Amnis Corporation, Merck-Millipore). Statistical significance was analyzed by Student's *t*-test ($p < 0.05$).

Antimicrobial Assay. Bacteria strains were purchased from Institut Pasteur-CRBIP (Paris). The technique used was based on a method published by the National Committee of Laboratory Safety and Standards (NCLSS) in 1997.[21] Products dissolved in DMSO (not exceeding 5%, total volume) were incubated with the bacterial strains, three marine [*Shewanella baltica* (CIP 105850T), *Aeromonas salmonicida* subsp. *salmonicida* (CIP 103209T), and *Vibrio anguillarum* (CIP 63.36T)], a Gram-positive (*Micrococcus luteus*, CIP A270), and a Gram-negative (*Escherichia coli*, CIP 54.8) strain, in 96-well plates (Merck) in PB medium, at 37 °C for 24 h, with stirring. Assays were carried out in triplicate, and the results averaged. Growth was evaluated by reading optical density (630 nm). When an activity was detected (absence of growth), a sample of the medium was transferred to rich solid medium (Petri dishes) to establish the effect (bacteriostatical or bactericidal effect).

■ ASSOCIATED CONTENT

● Supporting Information

The Supporting Information is available free of charge.

NMR measurement conditions, 1D (^{1}H,^{13}C, DEPT) and 2D (COSY, HOHAHA, HSQC, HMBC) NMR spectra, HPLC chromatograms of the Marfey's analysis, and retention times (min) of standard and natural Marfey's *N*-Me-Ile derivatives (PDF)

■ AUTHOR INFORMATION

Corresponding Author

*Tel: +33 4 68 662074. Fax: +33 4 68 662223. E-mail: banaigs@univ-perp.fr.

ORCID

Eva Alonso: 0000-0002-1131-6575

Bernard Banaigs: 0000-0003-3473-4283

Present Addresses

[□]SAS AkiNaO, Perpignan, France.

[▽]Université de Fribourg, Switzerland.

[○]DSM Nutritional Products, Columbia, Maryland 21045, United States.

Author Contributions

[#]A. Levert, R. Alavariño, and L. Bornancin contributed equally to this work.

Notes

The authors declare no competing financial interest.

■ ACKNOWLEDGMENTS

Financial support for this research was provided by La Ligue Contre le Cancer (Comité des Pyrénées-Orientales) (B.B.) and Heriot-Watt University's multidisciplinary Ph.D. and the French Government's Scientific Scholarship programs (A.M.B). P.C.W. acknowledges the EPSRC for provision of an Advanced Research Fellowship (GR/A11311/01). The authors are indebted to (1) Dr. M. Zubia, Université de Polynésie Française, Tahiti, French Polynesia, for morphological identification and phylogenetic analysis; (2) C. Moriou-Chesné, ICSN-CNRS, Gif/Yvette, France, for $[\alpha_D$ measurements; (3) Dr. W. T. Beck, St. Jude Children's Research Hospital, Memphis, TN, USA, for provision of the acute lymphoblastic leukemia cell line CCRF-CEM; (4) Dr. B. Delesalle (Ecole Pratique des Hautes Etudes, Perpignan, France) and Prof. C. Payri (Université de la Polynésie Française, Tahiti, French Polynesia), for organizing access to *L. majuscula* material for this study; and (5) Dr. G. Burgess, Heriot-Watt University, Edinburgh, UK, for access to his antimicrobial activity assay. Chromatographic, spectroscopic, and structural analyses were performed using the facilities of the Biodiversité et Biotechnologies Marines platform at the University of Perpignan (Bio2Mar, http://bio2mar.obs-banyuls.fr).

■ REFERENCES

(1) (a) Moore, R. E.; Banarjee, S.; Bornemann, V.; Caplan, F. R.; Chen, J. L.; Corley, D. G.; Larsen, L. K.; Moore, B. S.; Patterson, G. M. L.; Paul, V. J.; Stewart, J. B.; Williams, D. E. *Pure Appl. Chem.* **1989**, *61*, 521−524. (b) Moore, R. E. *J. Ind. Microbiol.* **1996**, *16*, 134−143.

(2) (a) Rinehart, K. L.; Harada, K.; Namikoshi, M.; Chen, C.; Harvis, C. A.; Munro, M. H. G.; Blunt, J. W.; Mulligan, P. E.; Beasley, V. R.; Dahlem, A. *J. Am. Chem. Soc.* **1988**, *110*, 8557−8558. (b) Jaspars, M.; Lawton, L. A. *Curr. Opin. Drug Discovery Devel.* **1998**, *1*, 77−84.

(3) (a) Gerwick, W. H.; Tan, L. T.; Sitachitta, N. *Alkaloids Chem. Biol.* **2001**, *57*, 75−184. (b) Burja, A.; Banaigs, B.; Abou-Mansour, E.; Burgess, J.; Wright, P. *Tetrahedron* **2001**, *57*, 9347−9377.

(4) Nogle, L. M.; Williamson, R. T.; Gerwick, W. H. *J. Nat. Prod.* **2001**, *64*, 716−719.

(5) Nogle, L. M.; Okino, T.; Gerwick, W. H. *J. Nat. Prod.* **2001**, *64*, 983−985.

(6) Davies-Coleman, M. T.; Dzeha, T. M.; Gray, C. A.; Hess, S.; Pannell, L. K.; Hendricks, D. T.; Arendse, C. E. *J. Nat. Prod.* **2003**, *66*, 712−715.

(7) Nogle, L. M.; Marquez, B. L.; Gerwick, W. H. *Org. Lett.* **2003**, *5*, 3−6.

(8) Williams, P. G.; Moore, R. E.; Paul, V. J. *J. Nat. Prod.* **2003**, *66*, 1356−1363.

(9) (a) Luesch, H.; Yoshida, W. Y.; Moore, R. E.; Paul, V. J. *J. Nat. Prod.* **2000**, *63*, 1437−1439. (b) Milligan, K. E.; Marquez, B. L.; Williamson, R. T.; Gerwick, W. H. *J. Nat. Prod.* **2000**, *63*, 1440−1443.

(10) Luesch, H.; Yoshida, W. Y.; Moore, R. E.; Paul, V. J.; Corbett, T. H. *J. Am. Chem. Soc.* **2001**, *123*, 5418−5423.

(11) Sitachitta, N.; Williamson, R. T.; Gerwick, W. H. *J. Nat. Prod.* **2000**, *63*, 197−200.

(12) Nogle, L. M.; Gerwick, W. H. *J. Nat. Prod.* **2002**, *65*, 21−24.

(13) (a) Luesch, H.; Pangilinan, R.; Yoshida, W. Y.; Moore, R. E.; Paul, V. J. *J. Nat. Prod.* **2001**, *64*, 304−307. (b) Montaser, R.; Paul, V. J.; Luesch, H. *Phytochemistry* **2011**, *16*, 2068−2074.

(14) Bunyajetpong, S.; Yoshida, W. Y.; Sitachitta, N.; Kaya, K. *J. Nat. Prod.* **2006**, *69*, 1539−1542.

(15) (a) Tripathi, A.; Puddick, J.; Prinsep, M. R.; Peng Foo Lee, P.; Tong Tan, L. *J. Nat. Prod.* **2009**, *72*, 29−32. (b) Tripathi, A.; Puddick, J.; Prinsep, M. R.; Peng Foo Lee, P.; Tong Tan, L. *Phytochemistry* **2010**, *71*, 307−311.

(16) (a) Tripathi, A.; Puddick, J.; Prinsep, M. R.; Rottmann, M.; Tan, L. T. *J. Nat. Prod.* **2010**, *73*, 1810−1814. (b) Tripathi, A.; Puddick, J.; Prinsep, M. R.; Rottmann, M.; Ping Chan, K.; Yu-Kai Chen, D.; Tong Tan, L. *Phytochemistry* **2011**, *72*, 2369−2375.

(17) Nakao, Y.; Yoshida, W. Y.; Szabo, C. M.; Baker, B. J.; Scheuer, P. J. *J. Org. Chem.* **1998**, *63*, 3272−3280.

(18) (a) Fujii, K.; Ikai, Y.; Mayumi, T.; Oka, H.; Suzuki, M.; Harada, K. *Anal. Chem.* **1997**, *69*, 3346−3352. (b) Fujii, K.; Ikai, Y.; Oka, H.; Suzuki, M.; Harada, K. *Anal. Chem.* **1997**, *69*, 5146−5151.

(19) Boudreau, P. D.; Byrum, T.; Liu, W. T.; Dorrestein, P. C.; Gerwick, W. H. *J. Nat. Prod.* **2012**, *75*, 1560−1570.

(20) Hellio, C.; De La Broise, D.; Dufosse, L.; Le Gal, Y.; Bourgougnon, N. *Mar. Environ. Res.* **2001**, *52*, 231−247.

(21) National Commitee for Clinical Laboratory Standards. Methods for Dilution Antimicrobial Susceptibility Tests for Bacteria that Grow Aerobicaly. Approved Standards. NCCLS Document M7-A4 4th ed.;Vilanova, PA, 1997.

(22) Lockshin, R. A.; Zakeri, A.; Tilly, J. L. *When Cells Die: A Comprehensive Evaluation of Apoptosis and Programmed Cell Death*; Wilsey-Liss: New York, 1998.

(23) (a) Voronina, E.; Wessel, G. M. *Mol. Reprod. Dev.* **2001**, *60*, 553−561. (b) Pellerito, C.; D'Agati, P.; Fiore, T.; Mansueto, C.; Mansueto, V.; Stocco, G.; Nagy, L.; Pellerito, L. *J. Inorg. Biochem.* **2005**, *99*, 1294−305.

(24) Philippe, L.; Tosca, L.; Zhang, W. L.; Piquemal, M.; Ciapa, B. *Apoptosis* **2014**, *19*, 436−450.

(25) Poon, I. K.; Hulett, M. D.; Parish, C. R. *Cell Death Differ.* **2010**, *17*, 381−397.

(26) Hoffmann, L.; Demoulin, V. *Belgian J. Bot.* **1991**, *124*, 82−88.

(27) Tacker, R. W.; Paul, V. J. *Appl. Environ. Microbiol.* **2004**, *70*, 3305−3312.

(28) Hanssen, K. O.; Andersen, J. H.; Stiberg, T.; Eng, R. A.; Svenson, J.; Geneviere, A. M.; Hanssen, E. *Anticancer Res.* **2012**, *32*, 4287−4297.